Trimeric ring-like structure of ArsA ATPase

Hong-Wei Wang[a], Ying-Jie Lu[a], Lin-Jiang Li[b], Susen Liu[b], Da-Neng Wang[c], Sen-fang Sui[a,*]

[a] *State Key Laboratory of Biomembrane & Membrane Biotechnology, Department of Biological Sciences & Biotechnology, Tsinghua University, Beijing 100084, PR China*
[b] *State Key Laboratory of Biomembrane & Membrane Biotechnology, Institute of Zoology, Academia Sinica, Beijing 100080, PR China*
[c] *Skirball Institute of Biomolecular Medicine, New York University Medical Center, New York, NY 10016, USA*

Received 15 December 1999; received in revised form 7 February 2000

Edited by Matti Saraste

Abstract ArsA protein is the soluble subunit of the Ars anion pump in the *Escherichia coli* membrane which extrudes arsenite or antimonite from the cytoplasm. The molecular weight of the subunit is 63 kDa. In the cell it hydrolyzes ATP, and the energy released is used by the membrane-bound subunit ArsB to transport the substrates across the membrane. We have obtained two-dimensional crystals of ArsA in the presence of arsenite on negatively-charged lipid monolayer composed of DMPS and DOPC. These crystals have been studied using electron microscopy of negatively-stained specimens followed by image processing. The projection map obtained at 2.4 nm resolution reveals a ring-like structure with threefold symmetry. Many molecular assemblies with the same ring-shape and dimensions were also seen dispersed on electron microscopy grids, prepared directly from purified ArsA protein solution. Size-exclusion chromatography of the protein sample with arsenite present revealed that the majority of the protein particles in solution have a molecular weight of about 180 kDa. Based on these experiments, we conclude that in solution the ArsA ATPase with substrate bound is mainly in a trimeric form.

Key words: ArsA ATPase; Two-dimensional crystallization; Electron microscopy; Oligomerization

1. Introduction

Arsenite (+3 oxidation state of arsenic) is extremely toxic to most biological organisms, including prokaryotes, since it can react directly with the sulfhydryl groups of proteins and thus destroys their biological functions [1,2]. Many organisms have, therefore, developed systems that can detoxify arsenicals. In prokaryotic cells, plasmids encoding arsenite-resistance systems have been discovered [3,4]. The most important component of the transport system is found to be an ATP-coupled oxyanion pump in the cell membranes which catalyzes extrusion of arsenite and antimonite so that the intercellular concentration of the toxic substances is minimized [5]. The pump is a complex composed of two proteins, ArsA and ArsB, which are separately encoded by the *arsA* and *arsB* genes. ArsB is a 45 kDa integral membrane protein that is postulated to be the oxyanion translocation part of the pump. The 63 kDa soluble ArsA protein, on the other hand, is the catalytic subunit, with As(III)/Sb(III)-stimulated ATPase activity. It anchors with ArsB to form the arsenite anion pump in the membrane [6,7]. When over-expressed in *Escherichia coli* at high levels, the ArsA protein is mainly found in the cytosol, from which it can be purified and characterized [8,9].

During the past decade, much work has been done in studying the functions and biochemical properties of the ArsA protein. The protein consists of 583 amino acids. The N- and C-terminal halves of the polypeptide (referred to as A1 and A2, respectively) are homologous in sequence [10], with each half having a consensus sequence as the binding site of phosphoryl group of ATP. As an ATPase, ArsA is allosterically regulated by the trivalent arsenic or antimonic. In the presence of arsenite or antimonite, the ATPase activity of ArsA is increased greatly. It has been hypothesized that when the regulator As(III) or Sb(III) binds to the allosteric site, the ArsA ATPase undergoes a conformational change so that A1 and A2 domains within the same monomer make contact with each other to form a catalytic site of ATP hydrolysis at the interface between the two ATP binding sites [7]. There is evidence that the covalent coordination of As(III) or Sb(III) atoms with SH groups of cysteine residues Cys-113, Cys-172, and Cys-422 in the ArsA polypeptide leads to conformational changes in the protein which increases its ATPase activity [11,12]. It has been proposed that the conformational change also leads to changes in the oligomeric state of protein. Based on biochemistry and point mutation experiments, Rosen's group has proposed models describing changes in oligomeric state of ArsA in different conditions [7,11]. It is suggested that in the presence of arsenite or antimonite, ArsA aggregates into dimers while it is in the monomeric form in solution in the absence of the trivalent anions [13]. This is referred to as the dimer model in the current report.

Though extensive investigations on the functions and biochemical properties of the ArsA protein have been made, a full understanding of the arsenite-resistance mechanism in organisms is still lacking, largely due to the absence of direct structural information. Recently, Zhou et al. [14] have obtained three-dimensional crystals of ArsA, but the solution of the protein structure has not yet been reported. In the current work, we have examined the structure of ArsA on lipid layer and in solution by electron microscopy (EM) and size-exclusion chromatography. Using the lipid monolayer technique, we obtained the two-dimensional (2D) crystals of ArsA in the presence of arsenite on negatively charged lipids. From the electron micrographs of the negatively-stained 2D crystals, a projection map at 2.4 nm resolution was calculated. A trimeric ring-like structure of ArsA ATPase was seen. In addition, on EM grids directly prepared from solution of purified ArsA protein, the same ring-like structures as in the 2D crystals were observed by EM. Furthermore, the majority of

*Corresponding author. Fax: (86)-10-62784768.
E-mail: suisf@mail.tsinghua.edu.cn

PII: S0014-5793(00)01257-6

the protein particles were found to have a molecular weight of about 180 kDa in the solution containing arsenite, corresponding to ArsA trimers. Thus, we concluded that the ArsA ATPase is in trimeric form in solution in the presence of its allosteric substrate, contradictory to the dimer model [7,11,15].

2. Materials and methods

2.1. Purification of ArsA ATPase

The wild type ArsA protein was expressed and purified as described previously [16]. In short, *E. coli* strain SG20043 bearing plasmid R773 encoding the wild type ArsA protein (a kind gift from Dr. B.P. Rosen of Wayne State University) was inoculated and cultured in LB medium at 37°C. The over-production of the protein was induced by the addition of isopropyl-β-D-thiogalactoside (IPTG). The ArsA protein was purified sequentially through ion-change Q-Sepharose, affinity red agarose, and size-exclusion Sepharyl S-200 columns to more than 95% homogeneity and stored at −70°C until use. The purity of ArsA protein was checked by silver staining of samples separated by sodium dodecylsulfate–polyacrylamide gel electrophoresis (SDS–PAGE). The protein concentration was determined by a modification of the Lowry method [17]. The ATPase activity of the protein was measured from the release of inorganic phosphate according to Rosen et al. [8].

2.2. Size-exclusion HPLC of ArsA ATPase

The molecular weight of the ArsA ATPase oligomers in solution was measured by size-exclusion HPLC. 50 μl of protein sample of 1 mg/ml concentration was loaded onto a Shodex GS-403 analytical size-exclusion column equilibrated with 20 mM MOPS–KOH, pH 7.5, 1 mM DTT, 2.5 mM $MgCl_2$, 5 mM $NaAsO_2$, 200 mM Na_2SO_4, and developed at 0.5 ml/min. The system was powered with a Waters 600S solvent delivery system controlled by Millennium control and data-collection software and data collection was via a photodiode array detector (Waters, Milford, MA, USA). Chromatograms were extracted from the photodiode array data at a wavelength of 280 nm. The molecular weight of the ArsA oligomer was estimated by comparison with the retention times of a set of protein standards of known molecular weight: ovalbumin (43 kDa), albumin (67 kDa), alcohol dehydrogenase (150 kDa) and amylase (200 kDa). Each of these protein standards was run on HPLC individually.

2.3. 2D crystallization of ArsA ATPase on lipid monolayer

For 2D crystallization of ArsA protein, the monolayer technique developed by Uzgiris and Kornberg [18] was used. 15 μl of purified ArsA solution at a concentration of 10–20 μg/ml was added into a small Teflon well (4 mm in diameter and 0.5 mm in depth), in buffer containing 20 mM MOPS–KOH (pH 5.5–7.5), 2.5 mM $CaCl_2$ or $MgCl_2$, 5 mM $NaAsO_2$ and 1 mM DTT. Then a droplet of 0.5–1.0 μl lipid mixture composed of DMPS and DOPC in 1:5 molar ratio at a concentration of 1.0 mg/ml, dissolved in chloroform/methanol (3:1, v/v), was spread over the protein solution in the well. The Teflon well was then incubated in a humid atmosphere at room temperature for 24–48 h. The amount of lipid sample added to the well was much more than required to form a lipid monolayer. Thus, with the aperture effect, the lipid monolayer on the surface of protein solution reached its highest pressure. The protein molecules may be adsorbed to the negatively charged lipid layers by electrostatic force. As the surface density of the protein molecules rises up they may arrange themselves laterally into 2D crystals due to favorable interactions between the protein molecules and the fluidity of the lipid layers.

2.4. EM and image processing

After incubation in the small Teflon well for proper period, the lipid monolayers with 2D crystals on them were picked up on hydrophobic carbon-coated EM grids. Briefly, the grids were placed horizontally by forceps onto the film at the air/water interface and picked up after they reached the monolayer. Blotted off the residual solution on the grids, they were negatively stained with 1–2% uranyl acetate for 2–3 min. For those single molecules of ArsA ATPase, a drop of purified protein solution with a concentration of about 10 μg/ml was adsorbed on carbon-coated EM grids for about 1 min then negatively stained with uranyl acetate.

EM samples were examined and data collection was done in a JEOL CX-200 transmission electron microscope. 2D crystals of ArsA were photographed at a magnification from 40 000–60 000 onto Kodak SQ-163 film. Judged by optical diffraction, only films with the best crystallinity and suitable defocus were selected and digitized with the AGFA DUOSCAN camera system in a step size of about 13 μm/pixel. The calculated Fourier transform of the image was indexed using SPECTRA program [19]. Subsequent processing steps were all done using the MRC Image Processing Package [20], including lattice refinement, lattice unbending, and amplitude and phase extraction. The phase residuals of crystals were calculated for different layer groups by the ALLSPACE program [21]. The final projection map was calculated using the CCP4 Package [22].

2.5. Materials and reagents

MOPS was purchased from Merck. DTT were purchased from Promega. Phospholipids DMPS and DOPC were purchased from

Table 1
Phase residuals (°) of image 6295 calculated for 17 layer groups by ALLSPACE

Layer group		Phase residue (no.) vs. other spots (90° random)		Phase residue (no.) vs. theoretical (45° random)		Target residual based on statistics taking the Friedel weight into account
1	*p*1	17.1	32	12.3	32	–
2	*p*2	25.7[a]	16	12.9	32	24.6
3b	*p*12_*b*	61.8	9	40.1	6	19.6
3a	*p*12_*a*	64.3	8	49.5	4	19.0
4b	$p12_1$_*b*	39.6	9	4.1	6	19.6
4a	$p12_1$_*a*	51.2	8	1.0	4	19.0
5b	*c*12_*b*	61.8	9	40.1	6	19.6
5a	*c*12_*a*	64.3	8	49.5	4	19.0
6	*p*222	70.5	33	12.9	32	20.7
7b	$p222_1$_*b*	48.3	33	13.0	32	20.7
7a	$p222_1$_*a*	39.6	33	12.9	32	20.7
8	$p22_12_1$	55.1	33	15.1	32	20.7
9	*c*222	70.5	33	12.9	32	20.7
10	*p*4	56.9	36	13.1	32	20.4
11	*p*422	59.0	80	12.9	32	18.6
12	$p42_12$	49.1	80	16.0	32	18.6
13	*p*3	7.4[b]	30	–	–	17.1
14	*p*312	18.2[b]	69	1.4	6	17.4
15	*p*321	61.3	73	53.8	14	17.8
16	*p*6	58.9	76	44.4	32	18.7
17	*p*622	61.8	158	44.4	32	17.9

[a]To be considered.
[b]Acceptable.

Sigma. Q-Sepharose, reactive red 120-agarose (type 3000-CL) columns were purchased from Sigma. Sephacryl S-200 (fine) columns were purchased from Pharmacia. All the other reagents were purchased locally in Beijing.

3. Results

3.1. 2D crystallization of ArsA ATPase on DMPS/DOPC monolayer

Samples were picked up to grids and examined by EM at different time intervals in order to check crystal formation. 2D crystals of purified ArsA were obtained on negatively charged DMPS/DOPC (1:5 in molar ratio), using the lipid monolayer 2D crystallization technique [18], when incubated for about 48 h at room temperature. The crystallization buffer contained 20 μg/ml ArsA in 20 mM MOPS–KOH buffer (pH 7.5) with the addition of 2.5 mM $MgCl_2$, 5 mM $NaAsO_2$ and 1 mM DTT.

During the 2D crystallization of ArsA on negatively charged DMPS/DOPC monolayer, keeping the protein in its stable and homogeneous conformation is one of the key factors. We found that the presence of DTT in solution is essential to keep the proteins stable. In its absence, no well-defined structures but only large amount of aggregates, probably composed of denatured proteins, were observed on the monolayer (data not shown). As the specific allosteric ligand of ArsA, arsenite or antimonite leads the ATPase to a conformation with higher activity [11,12]. Thus arsenite was added to the protein solution in order to keep proteins in fairly homogeneous conformation.

The ionic strength and pH of the solution are also important factors for 2D crystallization of the ArsA proteins on monolayer mediated by electrostatic adsorption. Buffers containing different concentrations of ions and with different pH values were tried in our work. +2 cations were found to be essential for the formation of 2D crystals of ArsA on negatively-charged DMPS/DOPC monolayer. In the presence of 2.5 mM calcium, 2D crystals of ArsA in a small area were obtained on DMPS/DOPC monolayer incubated at room temperature over 48 h. When the calcium was replaced with magnesium, well-ordered 2D crystals measuring up to several micrometers were obtained at the room temperature over 24 h (Fig. 1a). Variations of the pH from 5.5–7.5 were found to have little effect on the formation of 2D ArsA crystals.

3.2. Trimeric ring-like structure of ArsA obtained from 2D crystals by EM and image processing

Structural data from 2D ArsA crystals were collected by EM followed by image processing. Several hundred pictures were recorded from different crystals and six of them were processed. The Fourier transform showed a hexagonal pattern (Fig. 1b). After lattice unbending of the images using the MRC programs, the lattice parameters of the unit cell were

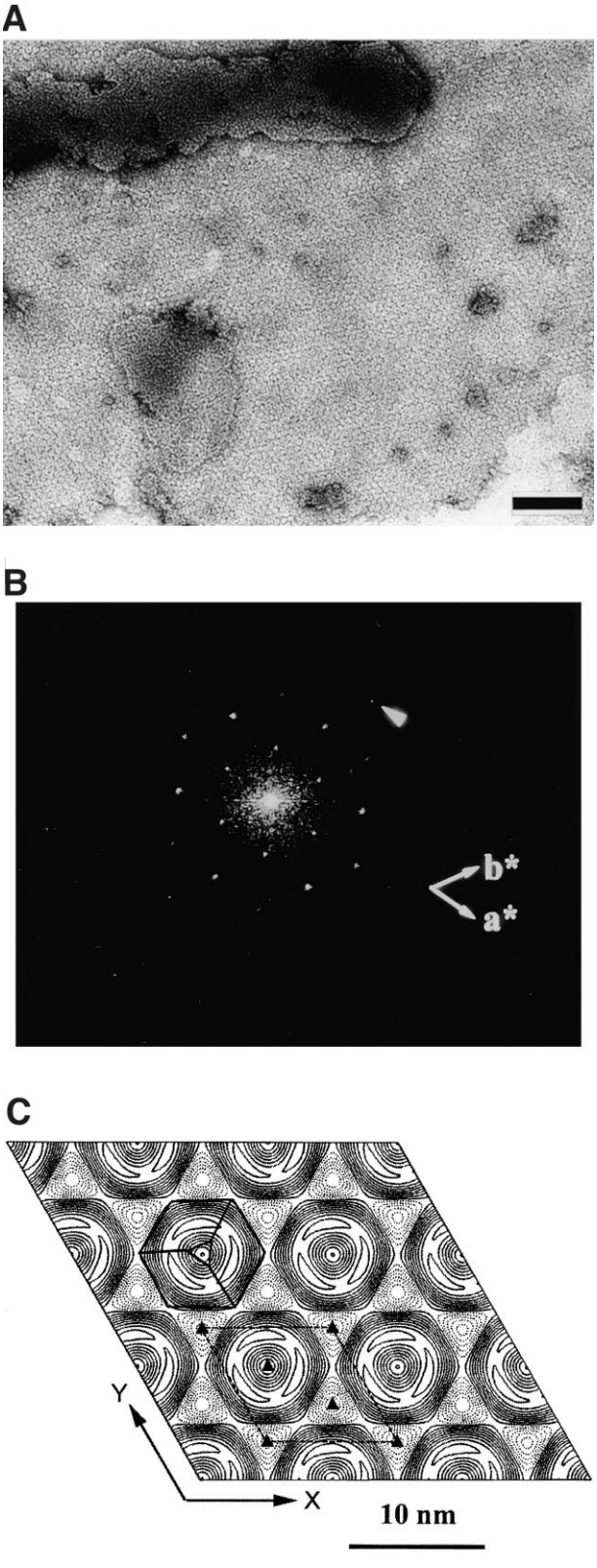

→

Fig. 1. EM and image processing of 2D ArsA crystals. A: Electron micrograph of a negatively-stained 2D of ArsA grown on negatively-charged DMPS/DOPC (1:5 in molar ratio) monolayer. The crystallization buffer contained 20 μg/ml ArsA in 20 mM MOPS–KOH buffer (pH 7.5) with the addition of 2.5 mM $MgCl_2$, 5 mM $NaAsO_2$, 1 mM DTT when incubated for about 48 h at room temperature. The crystals are found to possess *p*3 layer group symmetry. B: The computed diffraction pattern from the original image. The (−1,3) reflection at a resolution of 3.1 nm is indicated by an arrowhead. C: Projection map from ArsA 2D crystals by EM and image processing, averaged from six images with threefold symmetry imposed. One unit cell is indicated. The trimeric ring-like structure of 8.5 nm in diameter is seen. The possible way of assembly of three monomers in one ring is indicated by the boat-shaped boxes. Scale bar in (A) represents 100 nm.

determined to be $a = b = 9.6$ nm and $\gamma = 120°$. We used the ALLSPACE program [21] to calculate the internal phase residual of each of the 17 possible layer group symmetries, and the results for a typical image (film no. 6295, in this case) are listed in Table 1. The four layer groups with the internal phase residual lower than 30° are *p*1, *p*2, *p*3, and *p*312. The crystals clearly had a symmetry higher than *p*1. The phase residual of the six images for *p*3 layer group ranged from 7.4–23.3°, with the average being 16.4°. The averaged phase residuals for the *p*2 and *p*312 layer groups, on the other hand, were 31.0 and 26.0°, respectively. For the *p*6 layer group the average was 49.8°, even though the intensities of the calculated diffraction pattern (Fig. 1b) showed hexagonal symmetry. We therefore concluded that the 2D crystals of ArsA have a *p*3 layer group symmetry. The final projection map with the threefold symmetry imposed was calculated at a resolution of 2.4 nm, as shown in Fig. 1c.

In the projection map, we can see clearly one ring-like structure per unit cell, with an outer diameter of about 8.5 nm and a central stain-excluding area of 1.5 nm across (Fig. 1c). The structure shows a hexagonal shape and has three high electron density regions that are evenly distributed along the ring. One structure interacts with its six neighboring rings via the vertexes of the hexagon. The threefold symmetry of the ArsA assembly, including the overall hexagonal shape and the presence of three high-density regions, indicates that there may be three monomers in the assembly on lipid layer. The monomers are about 5×8 nm in projection as shown in Fig. 1c. The ring-like structures pack in the lattice in a relatively dense way.

3.3. *Trimeric structure of ArsA in solution observed by EM and size-exclusion chromatography*

The structure of ArsA ATPase in the solution containing arsenite was examined by EM of negatively-stained protein particles that was adsorbed onto the carbon film on EM grids. Many ring-like particles with a diameter of 8–10 nm were observed (Fig. 2). The ring-like structure are of the similar size and shape as those observed in the projection map from 2D crystals (Fig. 1c). In fact, such dispersed ring-like structures sometimes were also observed on DMPS/DOPC monolayer under the same condition for 2D crystallization (data not shown). This indicates that the ArsA protein in solution and in 2D crystals adopt the same oligomeric state, most likely a trimer.

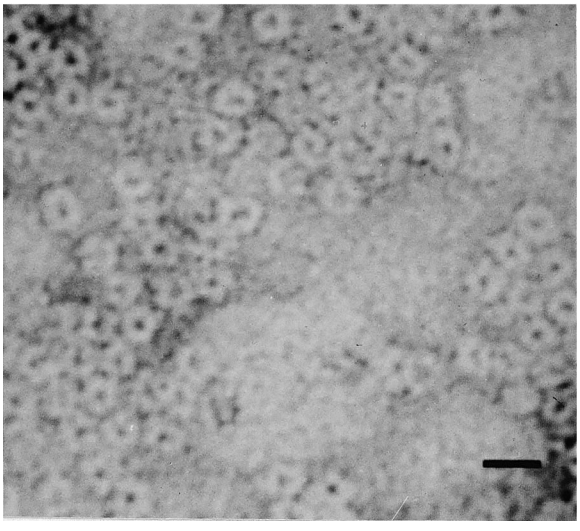

Fig. 2. Dispersion of ArsA ATPase particles in solution observed under electron microscope after negative staining. Ring-like structures of 8–10 nm across, similar to those seen in projection map from 2D crystals (Fig. 1c), are visible. The scale bar represents 10 nm.

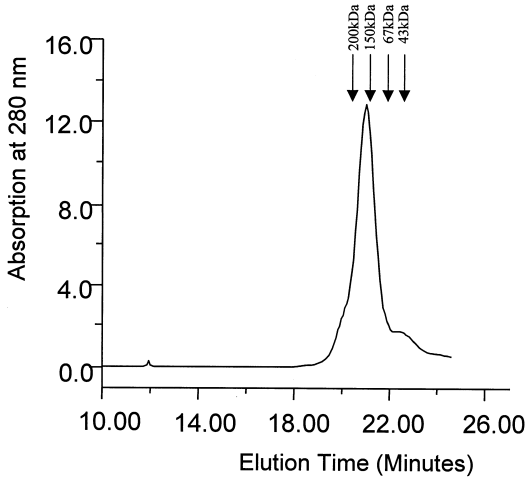

Fig. 3. The elution curve of ArsA ATPase with arsenite bound. Most of the protein is in a trimeric form, with a molecular weight of 180 kDa. Indicated by arrows are the retention times of protein standards: ovalbumin (43 kDa), albumin (67 kDa), alcohol dehydrogenase (150 kDa) and amylase (200 kDa). The void volume is at 12 min.

To determine molecular weight and hence, the exact oligomeric state, of the ArsA protein in solution, size-exclusion HPLC of purified ArsA protein was performed. In the presence of arsenite, the major peak of ArsA ATPase was found to have a molecular weight of 180 (±10) kDa (Fig. 3). The majority of the ArsA protein in solution, therefore, is indeed in a trimeric form, in agreement with the results from EM (Figs. 1c and 2). The small shoulder eluted after the trimers probably represents the monomeric ArsA protein of 63 kDa.

4. Discussion

4.1. *Oligomeric state of ArsA*

By 2D crystallization, EM and size-exclusion HPLC, we have shown the ArsA protein, in the presence of arsenite, adopts a trimeric form both in solution and on lipid layer. The trimer has a ring-like structure, with a diameter of 8.5 nm. Each monomer has two symmetrical halves, most likely representing the A1 and A2 sub-domains of the N- and C-terminus of the polypeptide.

The cytosolic part of the Ars pump, ArsA ATPase is fairly well characterized in the past decade on its biochemical properties in soluble form. However, up until now there are still no evident data to give direct structural information of the protein. Some investigators have tried in to study the structure of ArsA by indirect methods. The substrate-induced aggregation of the protein was found a significant property of ArsA ATPase. In 1991, Hsu et al. did systemic work on the protein's quaternary structure in solution [13]. By several types of techniques, they concluded that ArsA ATPase forms a dimeric structure in the presence of its allosteric substrate, arsenite or antimonite, while in the absence of the substrates, the pro-

tein exist in a monomeric form. Based on these results, models on the ArsA ATPase's conformation and structure changes regulated by the allosteric ligands were built [7,11]. The structure of the Ars pump in the membrane was also predicted to be a complex composed of homodimeric ArsA and ArsB subunits [15].

In our current work, however, we found that the ArsA ATPase was a trimeric ring in its 2D crystals on negatively-charged lipid monolayer in the presence of arsenite. The proteins are adsorbed onto membranes by electrostatic force and laterally form into 2D crystals by the interactions between the molecules themselves. High ionic strength in the buffer inhibits the adsorption of proteins on the monolayer. This suggests that there is no specific interaction of ArsA proteins with DMPS/DOPC monolayer. The observation of a large amount of the same single rings on membrane and protein solution supports this conclusion. This means that the ArsA ATPase in solution is also in a trimeric aggregation state. This is further supported by the measurement of ArsA ATPase's molecular weight by size-exclusion HPLC in solution. The apparent discrepancies between Hsu's work [13] and our results deserve special attention.

In Hsu et al.'s work, they used enzyme inhibition kinetics, chemical cross-linking, and light scattering technique to study the oligomerization of ArsA ATPase in solution [13]. They found that 5′-*p*-fluorosulfonylbenzoyladenosine (FSBA), the adenine nucleotide analogue which can inhibit the ATP binding site on ATPases, inhibited its ATPase activity completely in a inhibitor to protein molar ratio of 1.23:1 in the absence of antimonite and 0.55:1 in the presence of antimonite. With the assumption that with one ATP-binding site inhibited by FSBA, the whole molecule loses its ATPase activity completely whether the molecule is a monomer or an oligomer, they concluded that in the presence of antimonite the ArsA is a homodimer. However, this assumption seemed to lack other evidence, given the possible presence of non-specific binding of FSBA to the molecules mentioned by the authors. The zero length chemical cross-linking that was used is very sensitive to detect the presence of oligomers but less accurate to determine the exact oligomeric state. In Hsu et al.'s work, they observed the dimeric cross-linked species with the addition of antimonite in the incubation buffer. This demonstrated the oligomerization in the presence of antimonite, but it may not be safe to conclude that the protein was a dimer. Two adjacent monomers in a trimer or tetramer may also be cross-linked. In fact, they found the presence of a small amount of larger cross-linked products. Similarly, light scattering is more reliable in detecting oligomers than measuring their exact molecular weights, particularly when the sample consists of a mixture of different oligomers. Therefore, we believe that the trimeric ArsA protein observed by EM and size-exclusion HPLC is a more realistic oligomeric state of the protein when arsenite is present.

The functional Ars pump in membranes needs the assembly of ArsA and ArsB into a complex. What we reported here is just the structure ArsA in solution but not the membrane bound form. The exact quaternary structure of the complex, especially the stoichiometry of ArsA and ArsB in the complex, still needs further investigation.

4.2. The structure of ArsA monomer

The current projection map of ArsA trimer at 2.4 nm resolution (Fig. 1c) does not reveal much of the internal structure of the ArsA monomer. However, The phase residual of the images for the *p*312 layer group (Table 1), 26.0° in average for the six images processed, is relatively low and much smaller than the random value for this symmetry. This indicates that the 2D crystals of ArsA possess a pseudo-twofold axis in the crystal plane. This is consistent with the sequence homology observed between the two halves of the polypeptide, A1 and A2, and implies that the two halves of the monomer to have similar structures. The recently reported three-dimensional crystals belong to the *I*222 space group and also show pseudo-$I4_222$ symmetry [14]. The authors also attribute the pseudo-fourfold axis to internal symmetry of the ArsA molecule.

4.3. Comparison with other ATPase pumps

As the core machinery of the arsenite resistance system in bacteria, the arsenite pump is distinct with all the currently well-characterized ATPase pumps [23]. Until today, three families of ion-translocating ATPase pumps have been identified: the F_oF_1-ATPase in the bacterial, mitochondrial, and chloroplast membrane; the vacuolar proton pumps found in plant and fungal tonoplasts; the E_1E_2 cation-translocating ATPase such as the sarcoplasmic reticulum Ca^{2+}-ATPase and the plasma membrane Na^+/K^+-ATPase. Our projection map is very different from any known structure of any of these three ATPase protein families [24,25]. Since arsenite and antimonite have distinct properties from hydrogen ions and cations, the mechanism of their translocation through membranes must be different from the other types of ion pumps.

Comparison with the known structure of another ATP-driven pump reveals interesting insights. The structure of the ATP binding subunit HisP of the histidine transporter from *E. coli* has been determined by X-ray crystallography [26]. The protein is a member of the ATP binding cassette (ABC) transporter family. HisP protein consists of a homodimer of two 25 kDa polypeptides, each with one nucleotide binding pocket. Inspections of the X-ray model of HisP protein and the projection map of ArsA (Fig. 1c) reveal interesting similarities of the two proteins. In fact, both the shape and dimensions are so similar, that three copies of the X-ray structure of HisP (figure 1a of [25]) can actually be fitted nicely into the trimer in the projection map of ArsA (Fig. 1c). If we assume the thickness of the ArsA protein is also 4.5 nm, just like HisP, the ring-like structure in the ArsA projection map would yield a molecular weight of 190 kDa, consistent with the rest of our data and interpretations. Finally, we want to point out that, even though no sequence homology has been detected between the Ars protein and any ABC transporters, it is still not unlikely that they have similar structures and operate by similar mechanisms, at least in the ATP hydrolysis domains.

Acknowledgements: We thank Dr. Z.H. Zhou for help in installing the ICE Image Processing Package and Dr. R. Henderson providing the MRC programs to Tsinghua University. This work was supported by a grant from the China National Natural Science Foundation. D.N. Wang was a Whitehead Junior Faculty Fellow in Biological Sciences at New York University. His research was partly supported by the US National Institute of Health (DK53973).

References

[1] Knowles, F.C. (1982) Biochem. Int. 4, 647–653.

[2] Knowles, F.C. and Benson, A.A. (1983) Trends Biochem. Sci. 8, 178–180.
[3] Silver, S. and Keach, D. (1982) Proc. Natl. Acad. Sci. USA 79, 6114–6118.
[4] Mobley, H.L.T. and Rosen, B.P. (1982) Proc. Natl. Acad. Sci. USA 79, 6119–6122.
[5] Rosen, B.P., Bhattacharjee, H. and Shi, W.P. (1995) J. Bioenerg. Biomembr. 27, 85–91.
[6] Dey, S., Duo, D., Tisa, L.S. and Rosen, B.P. (1994) Arch. Biochem. Biophys. 311, 418–424.
[7] Li, J., Liu, S. and Rosen, B.P. (1996) J. Biol. Chem. 271, 25247–25252.
[8] Rosen, B.P., Weigel, U., Karkaria, C. and Gangola, P. (1988) J. Biol. Chem. 263, 3067–3070.
[9] Hsu, C.-M. and Rosen, B.P. (1989) J. Biol. Chem. 264, 17349–17354.
[10] Chen, C.-M., Misra, T.K., Silver, S. and Rosen, B.P. (1986) J. Biol. Chem. 261, 15030–15038.
[11] Bhattacharjee, H., Li, J., Ksenzenko, M.Y. and Rosen, B.P. (1995) J. Biol. Chem. 270, 11245–11250.
[12] Bhattacharjee, H. and Rosen, B.P. (1996) J. Biol. Chem. 271, 24465–24470.
[13] Hsu, C.-M., Kaur, P., Karkaria, C.E., Steiner, R.F. and Rosen, B.P. (1991) J. Biol. Chem. 268, 2327–2332.
[14] Zhou, T.Q., Rosen, B.P. and Gatti, D.L. (1999) Acta Cryst. D55, 921–924.
[15] Xu, C., Zhou, T., Kuroda, M. and Rosen, B.P. (1998) J. Biochem. 123, 16–23.
[16] Zhou, T.Q., Liu, S. and Rosen, B.P. (1995) Biochemistry 34, 13622–13626.
[17] Peterson, G.L. (1983) Methods Enzymol. 91, 95–119.
[18] Uzgiris, E.E. and Kornberg, R.D. (1983) Nature 301, 125–129.
[19] Hardt, S., Wang, B. and Schmid, M.F. (1996) J. Struct. Biol. 116, 68–70.
[20] Crowther, R.A., Henderson, R. and Smith, J.M. (1996) J. Struct. Biol. 116, 9–16.
[21] Valpuesta, J.M., Carrascosa, J.L. and Henderson, R. (1994) J. Mol. Biol. 240, 281–287.
[22] Collaborative Computational Project, Number 4 (1994) Acta Cryst. D50, 760–763.
[23] Petersen, P.L. and Carafoli, E. (1987) Trends Biochem. Sci. 12, 146–150.
[24] Abrahams, J.P., Leslie, A.G.W., Lutter, R. and Walker, J.E. (1994) Nature 370, 621–628.
[25] Zhang, P.J., Toyoshima, C., Yonekura, K., Green, N.M. and Stokes, D.L. (1998) Nature 392, 835–839.
[26] Hung, L.-W., Wang, I.X., Nikaido, K., Liu, P.-Q., Ames, G.F.-L. and Kim, S.-H. (1998) Nature 396, 703–707.